Spin observables in nucleon-deuteron scattering and three-nucleon forces

S. Ishikawa* and M. Tanifuji
Department of Physics, Science Research Center, Hosei University, Fujimi 2-17-1, Chiyoda, Tokyo 102-8160, Japan

Y. Iseri
Department of Physics, Chiba-Keizai College, Todoroki-cho 4-3-30, Inage, Chiba 263-0021, Japan
(Received 3 July 2002; published 24 October 2002)

Three-nucleon forces, which compose an up-to-date subject in few-nucleon systems, provide a good account of the triton binding energy and the cross section minimum in proton-deuteron elastic scattering. However, three-nucleon forces do not explain spin observables such as the nucleon and deuteron analyzing powers, suggesting serious defects in their spin dependence. We study the spin structure of nucleon-deuteron elastic amplitudes by decomposing them into spin-space tensors and examine effects of three-nucleon forces to each component of the amplitudes obtained by solving the Faddeev equation. Assuming that the spin-scalar amplitudes dominate the others, we derive simple expressions for spin observables in the nucleon-deuteron elastic scattering. The expressions suggest that a particular combination of spin observables in the scattering provides direct information on scalar, vector, or tensor component of the three-nucleon forces. These effects are numerically investigated by the Faddeev calculation.

DOI: 10.1103/PhysRevC.66.044005 PACS number(s): 21.45.+v, 21.30.−x, 24.70.+s

I. INTRODUCTION

In the last decade, a lot of investigations have been devoted to nucleon-deuteron (N-d) elastic scattering to provide valuable information on nuclear interactions such as an evidence of a three-nucleon force (3NF) [1–16]. In these studies, serious discrepancies between theoretical predictions with conventional models of two-nucleon force (2NF) and corresponding experimental data were found for some scattering observables in addition to the well known underbinding problem of the three-nucleon ($3N$) bound states. An example of the discrepancies is that calculated nucleon and deuteron vector analyzing powers are considerably smaller than those measured in a low-energy region, say $E_p \leq 20$ MeV [2,3,9,11,13,16–18]. Another example of the discrepancies is observed in the proton-deuteron (p-d) elastic cross sections around the minima of angular distributions, where the 2NF calculations underestimate the cross section systematically, when compared to the measured ones at intermediate energies $E_p = 60 - 150$ MeV [4,7,12]. The latter discrepancy has been solved by introducing a two-pion exchange three-nucleon force (2πE-3NF) with a cutoff parameter adjusted so as to reproduce the empirical binding energy of the triton [19]. However, the introduction of the 3NF provides only a small effect on the former discrepancy, or sometimes gives rise to worse agreements with experimental data on some spin observables [5–8,10,12,15]. We are, therefore, still far from the final understanding of nuclear interactions in the 3N system.

Since the difficulties are concerned with the spin observables, detailed investigations on the contribution of spin-dependent interactions in the observables will be required for improving the relevant interactions. Previously [20], we have analyzed the imaginary parts of neutron-deuteron (n-d) forward scattering amplitudes, which are transformed into combinations of total cross sections for polarized or unpolarized beams and targets by the use of the optical theorem. By decomposing the forward amplitudes according to their spin-space properties and examining the contributions of spin-dependent interactions to the components, we have succeeded in clarifying spin-dependent effects of the 3NF on combinations of the total cross sections. Being encouraged by such success, we will here develop the previous work to the case of N-d spin observables at finite scattering angles. As in Ref. [20], we will examine the contribution of a particular spin-dependent interaction on the observables by tagging ranks of related spin-space tensors on the scattering amplitude as described below, and then will study which observable characterizes the effect of the particular spin-dependent interaction.

For the tagging, we will decompose scattering amplitudes according to the tensorial property in the spin space. In such decomposition, where we obtain scalar amplitude, vector one, second-rank tensor one, and so on, each component specified by the tensor rank will describe the scattering by corresponding interactions: the scalar component will describe the scattering by central interactions, the vector one the scattering by spin vector interactions such as spin-orbit ones, and the second-rank tensor one the scattering by tensor interactions. In the following section, such decomposition of the scattering amplitude is performed in a model-independent way by the invariant amplitude method [21].

When the observables are described in terms of such decomposed amplitudes, one will be able to identify the contribution of the particular spin-dependent interaction by the help of the associated tensor rank. However, full expressions of the observables in terms of the decomposed scattering amplitudes are rather complicated. In Sec. III, we will show that the central interaction will dominate the scattering at low energies. Then the observables are described rather simply in an approximation neglecting second order terms of the vector and tensor amplitudes in the expressions. This approximation gives a clear insight into the role of each component of the interaction and one can obtain the information on the

*Email address: ishikawa@i.hosei.ac.jp

observables, which characterize the contribution of the component. Utilizing the results, typical observables such as the vector and tensor analyzing powers and spin correlation coefficients are fully analyzed by the Faddeev calculations in Sec. IV. In the analyses, investigations are particularly focused on the contributions of 3NFs to the observables, which include various spin effects and are decomposed into scalar effects, vector ones, and tensor ones. The incident energy is fixed to $E_N=3$ MeV, since at low energies below the deuteron breakup threshold, the Coulomb interaction can be treated exactly in the Faddeev calculation [22].

Matrix elements of a scattering T matrix in terms of the invariant amplitudes are given in Appendix A, and formulas of polarization transfer coefficients in the approximation are given in Appendix B for the convenience of applications of the theory.

II. *T* MATRIX AND TRANSITION AMPLITUDES

Let us describe a scattering T matrix $\boldsymbol{M}$ for the N-d scattering by specifying the elements by the z component of the deuteron spin ν_d and that of the nucleon spin ν_N as

$$\boldsymbol{M}=\begin{pmatrix} A & B & C & D & E & F \\ G & H & I & J & K & L \\ M & N & O & P & Q & R \\ R & -Q & -P & O & N & -M \\ L & -K & -J & I & H & -G \\ -F & E & D & -C & -B & A \end{pmatrix}, \tag{1}$$

where the row and column are designated by $(\nu_d=1,\nu_N=\frac{1}{2})$, $(\nu_d=1,\nu_N=-\frac{1}{2})$, $(\nu_d=0,\nu_N=\frac{1}{2})$, $(\nu_d=0,\nu_N=-\frac{1}{2})$, $(\nu_d=-1,\nu_N=\frac{1}{2})$, $(\nu_d=-1,\nu_N=-\frac{1}{2})$ from left to right for the initial state and from top to bottom for the final state. These matrix elements will explicitly be described by scattering amplitudes that have a particular tensorial property in the spin space. For that purpose, we will decompose $\boldsymbol{M}$ by spin-space tensors $\boldsymbol{S}_{K\kappa}$, where K and κ are the rank of the tensor and its z component,

$$\boldsymbol{M}=\sum_K \boldsymbol{M}_K, \quad \boldsymbol{M}_K=\sum_\kappa (-)^\kappa \boldsymbol{S}_{K-\kappa}\boldsymbol{R}_{K\kappa}. \tag{2}$$

Here, $\boldsymbol{R}_{K\kappa}$ is the counter part, a tensor in the coordinate space. Using Eq. (2), matrix elements of $\boldsymbol{M}_K$ are given [21] by

$$\begin{aligned}\langle \nu_N'\nu_d';\boldsymbol{k}_f|\boldsymbol{M}_K|\nu_N\nu_d;\boldsymbol{k}_i\rangle &= \sum_{s_is_f}(s_Ns_d\nu_N\nu_d|s_i\nu_i)(s_Ns_d\nu_N'\nu_d'|s_f\nu_f)(-)^{s_f-\nu_f} \\ &\times(s_is_f\nu_i-\nu_f|K\kappa)\sum_{l_i=K-K}^{K}[C_{l_i}(\hat{k}_i) \\ &\otimes C_{l_f=\overline{K}-l_i}(\hat{k}_f)]_\kappa^K F(s_is_fKl_i),\end{aligned} \tag{3}$$

where s is the spin of the related particle, $\boldsymbol{k}_i$ ($\boldsymbol{k}_f$) is the N-d relative momentum in the initial (final) state, $C_{lm}(\Omega)=[4\pi/(2l+1)]^{1/2}Y_{lm}(\Omega)$, and $\overline{K}=K$ for even K and $\overline{K}=K+1$ for odd K. The amplitude $F(s_is_fKl_i)$ is called the invariant amplitude due to the invariance under rotations of the coordinate axes and is a function of the center of mass energy and the scattering angle θ. In Eq. (3), while the geometrical part of the matrix element of $\boldsymbol{S}_{K-\kappa}$ is described by the Clebsch-Gordan coefficients using the Wigner-Eckart theorem and that of $\boldsymbol{R}_{K\kappa}$ is represented by $[C_{l_i}(\hat{k}_i)\otimes C_{l_f}(\hat{k}_f)]_\kappa^K$, their physical parts are included in $F(s_is_fKl_i)$, which represents the scattering by spin-space scalar interactions for $K=0$, the one by vector interaction for $K=1$, and so on.

For the N-d scattering, in which s_i and s_f are $\frac{1}{2}$ or $\frac{3}{2}$, K takes 0, 1, 2, and 3. For the components of the amplitude in Eq. (3), we will denote the scalar amplitudes ($K=0$), the vector ones ($K=1$), the tensor ones ($K=2$), and the third-rank tensor ones ($K=3$) as follows:

$$\begin{aligned} U_1&\equiv F\left(\frac{1}{2}\frac{1}{2}00\right), \\ U_3&\equiv F\left(\frac{3}{2}\frac{3}{2}00\right), \end{aligned} \tag{4}$$

$$\begin{aligned} S_1&\equiv[C_1(\hat{k}_i)\otimes C_1(\hat{k}_f)]_1^1 F\left(\frac{1}{2}\frac{1}{2}11\right), \\ S_2&\equiv[C_1(\hat{k}_i)\otimes C_1(\hat{k}_f)]_1^1 F\left(\frac{3}{2}\frac{1}{2}11\right), \\ S_3&\equiv[C_1(\hat{k}_i)\otimes C_1(\hat{k}_f)]_1^1 F\left(\frac{3}{2}\frac{3}{2}11\right), \\ S_4&\equiv[C_1(\hat{k}_i)\otimes C_1(\hat{k}_f)]_1^1 F\left(\frac{1}{2}\frac{3}{2}11\right), \end{aligned} \tag{5}$$

$$\begin{aligned} T_1(\kappa)&\equiv\sum_{l_i}[C_{l_i}(\hat{k}_i)\otimes C_{l_f}(\hat{k}_f)]_\kappa^2 F\left(\frac{3}{2}\frac{1}{2}2l_i\right), \\ T_2(\kappa)&\equiv\sum_{l_i}[C_{l_i}(\hat{k}_i)\otimes C_{l_f}(\hat{k}_f)]_\kappa^2 F\left(\frac{1}{2}\frac{3}{2}2l_i\right), \\ T_3(\kappa)&\equiv\sum_{l_i}[C_{l_i}(\hat{k}_i)\otimes C_{l_f}(\hat{k}_f)]_\kappa^2 F\left(\frac{3}{2}\frac{3}{2}2l_i\right) \\ &(\kappa=0,1,2), \end{aligned} \tag{6}$$

$$\begin{aligned} V(\kappa)&\equiv\sum_{l_i}[C_{l_i}(\hat{k}_i)\otimes C_{l_f}(\hat{k}_f)]_\kappa^3 F\left(\frac{3}{2}\frac{3}{2}3l_i\right) \\ &(\kappa=1,2,3). \end{aligned} \tag{7}$$

Here, U_1 and S_1 describe the scattering in the spin doublet state ($s_i=s_f=\frac{1}{2}$), U_3, S_3, $T_3(\kappa)$, and $V(\kappa)$ describe those in the spin quartet state ($s_i=s_f=\frac{3}{2}$), and S_2, S_4, $T_1(\kappa)$, and $T_2(\kappa)$ describe the doublet-quartet nondiagonal transitions. The time reversal theorem gives one relation,

$$S_4=-S_2, \tag{8}$$

for the vector amplitudes, four relations between the nine tensor amplitudes, and one relation between the three third-rank tensor amplitudes, although latter five relations are not used explicitly. These relations are equivalent to those given for $d+{}^3$He scattering in Ref. [23].

The matrix elements $A,\ldots,R$ are described in terms of the amplitudes $U_1,\ldots,V(3)$, whose explicit expressions are given in Appendix A. Solving Eqs. (A1)–(A18) in Appendix A inversely, we get the amplitudes $U_1,\ldots,V(3)$ in terms of $A,\ldots,R$ as follows:

$$U_1=\frac{2\sqrt{2}}{3}H-\frac{2}{3}I-\frac{2}{3}N+\frac{\sqrt{2}}{3}O,$$

$$U_3=A+\frac{1}{3}H+\frac{\sqrt{2}}{3}I+\frac{\sqrt{2}}{3}N+\frac{2}{3}O,$$

$$S_1=\frac{1}{3}(\sqrt{2}J-2K-P+\sqrt{2}Q), \tag{9}$$

$$S_2=-\frac{1}{6}(3\sqrt{2}G-3M+2J+\sqrt{2}K-\sqrt{2}P-Q),$$

$$S_3=\frac{1}{3\sqrt{10}}(3B+3\sqrt{2}C-3G-3\sqrt{2}M+2\sqrt{2}J+2K+4P+2\sqrt{2}Q),$$

$$S_4=-\frac{1}{6}(3\sqrt{2}B-3C+J-\sqrt{2}K+\sqrt{2}P-2Q), \tag{10}$$

$$T_1(0)=-\frac{2}{3}H-\frac{2\sqrt{2}}{3}I+\frac{\sqrt{2}}{3}N+\frac{2}{3}O,$$

$$T_2(0)=\frac{2}{3}H-\frac{\sqrt{2}}{3}I+\frac{2\sqrt{2}}{3}N-\frac{2}{3}O,$$

$$T_3(0)=A-\frac{1}{3}H-\frac{\sqrt{2}}{3}I-\frac{\sqrt{2}}{3}N-\frac{2}{3}O, \tag{11}$$

$$T_1(1)=-\frac{1}{2\sqrt{3}}(\sqrt{2}G-M-2J-\sqrt{2}K+\sqrt{2}P+Q),$$

$$T_2(1)=\frac{1}{2\sqrt{3}}(\sqrt{2}B-C-J+\sqrt{2}K-\sqrt{2}P+2Q),$$

$$T_3(1)=-\frac{1}{\sqrt{6}}(B+\sqrt{2}C+G+\sqrt{2}M), \tag{12}$$

$$T_1(2)=-\frac{1}{\sqrt{3}}(\sqrt{2}L-R),$$

$$T_2(2)=-\frac{1}{\sqrt{3}}(D-\sqrt{2}E),$$

$$T_3(2)=\frac{1}{\sqrt{6}}(\sqrt{2}D+E+L+\sqrt{2}R), \tag{13}$$

$$V(1)=\frac{1}{\sqrt{15}}(B+\sqrt{2}C-G-\sqrt{2}M-\sqrt{2}J-K-2P-\sqrt{2}Q),$$

$$V(2)=\frac{1}{\sqrt{6}}(L+\sqrt{2}R-\sqrt{2}D-E),$$

$$V(3)=F. \tag{14}$$

Intrinsic third-rank tensor interactions are unknown and possible third-rank tensor amplitudes may arise from higher orders of the vector and tensor interactions, which is supposed to have small contributions to the scattering. Then the third-rank tensor amplitudes will be neglected in later applications for simplicity.

When effective interactions are introduced by a *N-d* two-body model, one can directly relate the amplitude U_j, $T_j(\kappa=0,1,2)$, and S_j to the components of the model interactions, i.e., central ones, tensor ones, and spin-orbit ones. The example of the relation is given in Ref. [20]. Then the analyses in the following sections can be represented in terms of such effective interactions when necessary.

III. ANALYSES OF INVARIANT AMPLITUDES

In the present work, we have calculated the scattering amplitudes by solving the Faddeev equation in the coordinate space [24] with the Argonne V_{18} model (AV18) [25] for the input 2NF. The Coulomb interaction is included for the *p-d* scattering by the method described in Ref. [22]. The $3N$ partial wave states for which the 2NF acts are restricted to those with total two-nucleon angular momenta up to 2, and the total $3N$ angular momentum is truncated at 19/2. The accuracy of our calculations is examined by the comparison with variational calculations for the AV18 2NF with the pair correlated hyperspherical harmonics basis [26], whose results of the AV14 2NF [27] are considered as benchmarks for the *n-d* scattering [28] and the *p-d* scattering [29]. The agreement of the phase-shift parameters by both methods are found within a few percent deviation for all of thirty phase-shift parameters up to the $5/2^-$ state [22].

Calculated binding energy of the triton for the AV18 is 7.51 MeV, which is small compared to the empirical value of 8.48 MeV. An additional contribution of the 2πE-3NF is investigated by using the Brazil model (BR) [30], which

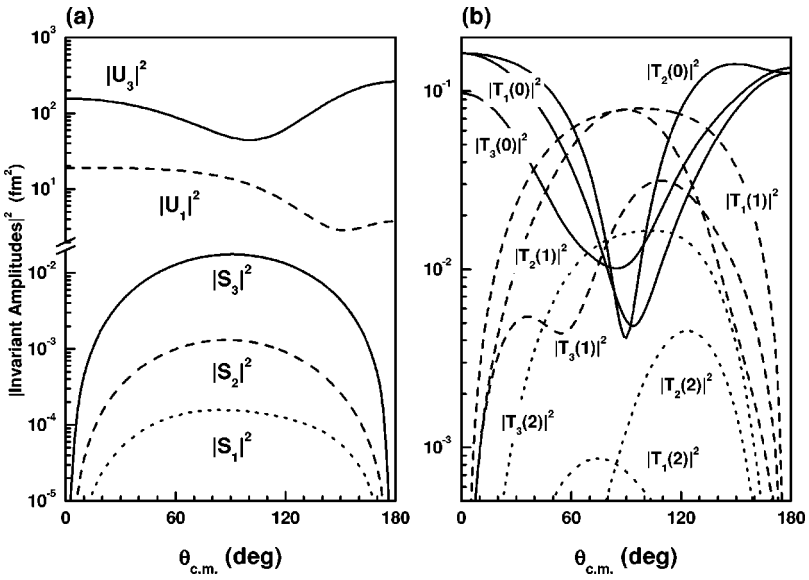

FIG. 1. The absolute squares of the scattering amplitudes U_1, U_3, S_1, S_2, and S_3 are shown in (a), and those of $T_1(\kappa)$, $T_2(\kappa)$, and $T_3(\kappa)$ for $\kappa=0,1,2$ are shown in (b). The curves are the Faddeev calculations with the AV18 for the *n-d* scattering at $E_n=3$ MeV.

gives 8.44 MeV for the triton binding energy in combination with AV18 (AV18+BR). Furthermore, we introduce two kinds of phenomenological models of the 3NF. One is for the study of the role of the central force part of the BR-3NF, which is simulated by a Gaussian type (GS) [14] as

$$V_{\text{GS-3}NF}=V_0^G\sum_{i\neq j\neq k}\exp\left\{-\left(\frac{r_{ji}}{r_G}\right)^2-\left(\frac{r_{ki}}{r_G}\right)^2\right\}. \quad (15)$$

Values of the parameters, which are determined so as to reproduce the empirical triton binding energy of 8.48 MeV in combination with AV18 (AV18+GS), are $r_G=1.0$ fm and $V_0^G=-45$ MeV. The other model of 3NF is the spin-orbit (SO) 3NF [31], which is adopted as an example of new spin vector interactions to account for the discrepancy in the vector analyzing powers,

$$V_{\text{SO-3}NF}=\frac{1}{2}W_0\exp\{-\alpha\rho\}\sum_{i<j}[\boldsymbol{l}_{ij}\cdot(\boldsymbol{\sigma}_i+\boldsymbol{\sigma}_j)]\hat{P}_{11}, \quad (16)$$

with $\rho^2=\frac{2}{3}(r_{12}^2+r_{23}^2+r_{31}^2)$ and $\hat{P}_{11}$ is the projection operator to the spin and isospin triplet state of the pair (i,j). For this interaction several parameter sets are suggested in Ref. [31], among which we take $\alpha=1.5$ fm^{-1} and $W_0=-20$ MeV. The SO-3NF gives a repulsive effect on the triton binding energy. The resultant binding energy for the SO-3NF with the BR-3NF (AV18+BR+SO) is 8.39 MeV.

We first calculate the magnitudes of the scalar, vector, and tensor amplitudes, for which the contributions of the 3NF are examined. Figure 1 shows as functions of the scattering angle the squares of the absolute magnitudes of the amplitudes, U_1, U_3, S_1, S_2, S_3, $T_1(\kappa)$, $T_2(\kappa)$, and $T_3(\kappa)$ ($\kappa=0,1,2$), obtained by the Faddeev calculation without the 3NF for the *n-d* scattering at $E_n=3$ MeV. There the magnitude of the quartet scattering amplitude U_3 is much larger than that of the doublet scattering amplitude U_1. Among the three vector amplitudes, the magnitude of the quartet scattering amplitude S_3 is much larger than other two, those of the doublet scattering S_1 and the doublet-quartet nondiagonal transition amplitude S_2. The magnitude of S_2 is larger than that of S_1. They have similar shapes in the angular distribution which have maxima around $\theta=90°$. The absolute squares of the tensor amplitudes, $T_1(0)$, $T_2(0)$, and $T_3(0)$ show similar angular dependence in a global sense. Other tensor amplitudes also have common characteristics in the angular distributions for $\kappa=1$ and $\kappa=2$, respectively, although in less grades than for $\kappa=0$. These properties of the vector and tensor amplitudes reflect the specific characters of the θ dependent factors in Eqs. (5) and (6), since the θ dependence of $F(s_i s_f K l_i)$ is weak at the present incident energy.

The contributions of the 3NFs on the *n-d* scattering amplitudes are shown in Fig. 2, where we have displayed the ratio of the magnitude of each amplitude calculated with the 3NF to that of the amplitude calculated without any 3NF. In the figure, the amplitude U_3 is little affected by the 3NFs, while U_1 receives large contributions from the BR-3NF as well as from the GS-3NF. The SO-3NF provides very small contributions to U_1. In more detail, the contribution of the BR-3NF to U_1 is considered to be mostly due to the central part of the interaction, because the magnitude and the angular distribution of the contribution are very similar to those of the GS-3NF. The vector amplitudes, S_1, S_2, and S_3, are influenced by the 3NFs, and particularly the SO-3NF produces large contributions to S_2 and S_3. The 3NF-effects on the tensor amplitudes are examined, for example, for the spin quartet scattering, where $T_3(0)$ and $T_3(1)$ are considerably affected by the BR-3NF but are very little affected by the GS-3NF or by the SO-3NF. The amplitude $T_3(2)$ is hardly affected by any 3NF studied. Such properties of the amplitudes will be reflected on the observables in the analyses in the following section.

IV. ANALYSES OF OBSERVABLES

In the preceding section, we observed that the scalar amplitudes are larger in magnitude than the vector and tensor amplitudes at the low energy. In this section, analytical ex-

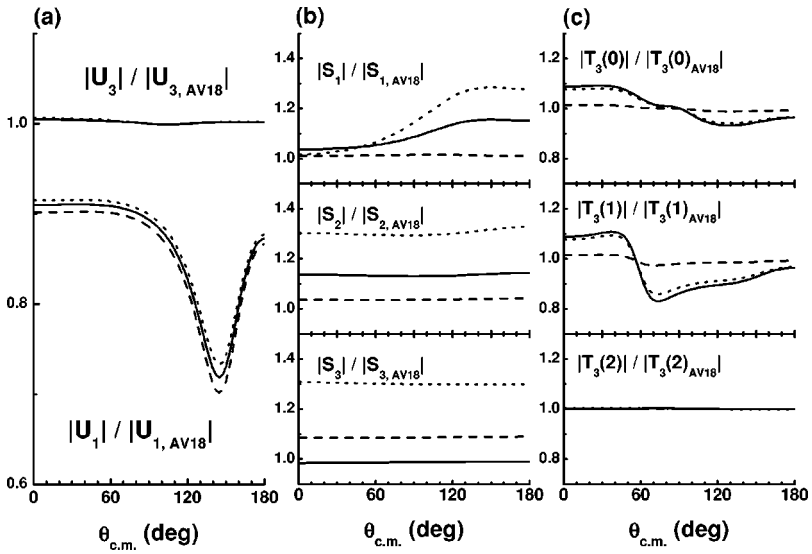

FIG. 2. The 3NF effects on the scattering amplitudes in the n-d scattering at $E_n=3$ MeV are shown by the ratio of the magnitude calculated with a 3NF to that without it for the scalar amplitudes (a), for the vector amplitudes (b), and for the tensor amplitudes in the spin quartet scattering with $\kappa=0,1,2$ (c). The solid curves denote the calculations for AV18+BR, the dashed curves for AV18+GS, and the dotted curves for AV18 +BR+SO.

aminations of N-d observables will be carried out in an approximation where we neglect the second order terms of the vector and tensor amplitudes in the observables. The results by this approximation, which we call the scalar amplitude dominance (SAD) approximation, are used as the guidelines for the numerical analyses of the observables with N-d amplitudes provided by the Faddeev calculations [22].

A. Differential cross section

The unpolarized differential cross section $\sigma(\theta)$ is expressed as

$$\sigma(\theta)=\frac{1}{6}N_R, \tag{17}$$

where N_R is defined as

$$N_R=\mathrm{Tr}(\boldsymbol{M}\boldsymbol{M}^\dagger), \tag{18}$$

and the factor 6 arises from the spin average in the initial state.

In the SAD approximation, N_R is given by

$$N_R=|U_1|^2+|U_3|^2. \tag{19}$$

Differences between fully calculated differential cross sections and those in the SAD approximation are less than 1%.

B. Vector analyzing powers

The vector analyzing powers of the proton and the deuteron, A_y and iT_{11}, are defined as

$$A_y=\frac{1}{N_R}\mathrm{Tr}(\boldsymbol{M}\sigma_y\boldsymbol{M}^\dagger), \tag{20}$$

$$iT_{11}=\frac{i}{N_R}\mathrm{Tr}(\boldsymbol{M}\tau_{11}\boldsymbol{M}^\dagger), \tag{21}$$

where $\tau_{11}=-(\sqrt{3}/2)(\tau_x+i\tau_y)$ and τ_x and τ_y are the x and y components of the spin vector operator of the deuteron.

In the SAD approximation,

$$A_y=\frac{4}{3N_R}\mathrm{Im}\left\{U_1\left(-\frac{1}{\sqrt{2}}S_1+2S_2\right)^* + U_3\left(\sqrt{2}S_2+\sqrt{\frac{5}{2}}S_3\right)^*\right\}, \tag{22}$$

$$iT_{11}=\frac{1}{N_R}\sqrt{\frac{2}{3}}\mathrm{Im}\{U_1(2S_1-\sqrt{2}S_2)^*+U_3(-S_2+\sqrt{5}S_3)^*\}. \tag{23}$$

These equations show that the scalar amplitudes and the vector ones dominantly govern the vector analyzing powers.

First we will numerically examine the validity of the SAD approximation in the vector analyzing powers, by comparing Eqs. (22) and (23) with the exact calculations. Figure 3 shows the comparison where the SAD approximation works very well, indicating the contributions of the neglected terms to be small. Therefore the approximation will have sufficient accuracy to obtain the guidelines for further calculations.

Next, we will examine the contributions of the related interactions in detail. Since the magnitude of U_3 is much larger than that of U_1 as seen in Fig. 1, one can expect the dominant contribution to the vector analyzing powers to arise from the U_3 terms of Eqs. (22) and (23), which are accompanied by two vector amplitudes S_2 and S_3. To extract the contribution of one of these amplitudes, we will eliminate the other by considering a linear combination of A_y and iT_{11}: the contribution of S_2 will be enhanced by the combination $A_y-(2/\sqrt{3})iT_{11}$ and that of S_3 by the combination $A_y+(4/\sqrt{3})iT_{11}$. Considering these features, we will investigate for the p-d scattering the contribution of the 2NF and the corrections due to the 3NF to the analyzing powers where the SO-3NF produces the dominant correction. As seen in Fig. 4, the Faddeev calculation with the AV18 does not reproduce the measured A_y and iT_{11}, while the calcula-

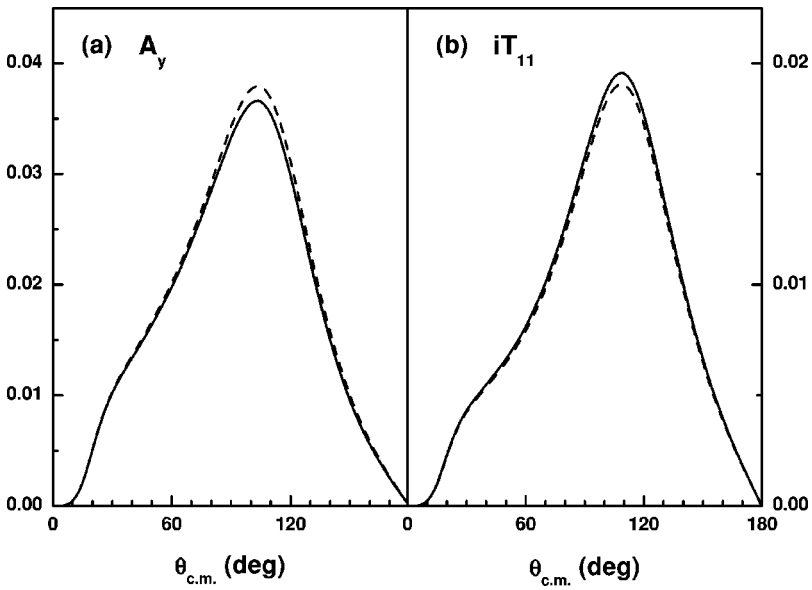

FIG. 3. The vector analyzing powers of protons A_y and deuterons iT_{11} for the p-d scattering at $E_p=3$ MeV by the exact calculations (solid curves) and by the SAD approximation (dashed curves) for AV18.

tion that includes the SO-3NF improves very much the agreement with the data for both of A_y and iT_{11} due to the large contribution of the SO-3NF to the amplitudes S_2 and S_3 as seen in Fig. 2. In the figure, the calculations are compared with the data for the combinations $A_y+(4/\sqrt{3})iT_{11}$ and $A_y-(2/\sqrt{3})iT_{11}$ obtained from those of A_y and iT_{11}, where the SO-3NF reproduces quite well the data of the former combination but the data of the latter are not sufficiently reproduced by the calculation, although the improvement of the agreement with the latter data is appreciable for the SO-3NF contribution. This means that the SO-3NF does not describe the amplitude S_2 sufficiently. Since the magnitude of S_2 is much smaller than that of S_3 as seen in Fig. 1, the inadequacy of the contribution of S_2 is masked by the contribution of S_3 in A_y and iT_{11}. Then, the linear combinations proposed here will provide more refined tests of the spin vector interaction than the analyzing powers themselves, at such low energies.

C. Spin correlation coefficients

In the previous paper [20], we have investigated the total cross sections of the n-d scattering for the unpolarized neutron and deuteron, for the transversal polarizations where the polarizations of the neutron and the deuteron are perpendicular to the z axis, and for the longitudinal polarizations where the polarizations of the neutron and the deuteron are parallel to the z axis, and have shown that linear combinations of these cross sections give information on $U_1(\theta=0)$ and $U_3(\theta=0)$, separately. To extend this idea to finite angles, we will investigate the spin correlation coefficients defined as

$$C_{\alpha,\beta}=\frac{1}{N_R}\mathrm{Tr}(\boldsymbol{M}\tau_\alpha\sigma_\beta\boldsymbol{M}^\dagger). \tag{24}$$

The spin correlation coefficient for the transversal polarizations will representatively be described by the average of $C_{x,x}$ and $C_{y,y}$, which is given in the SAD approximation as

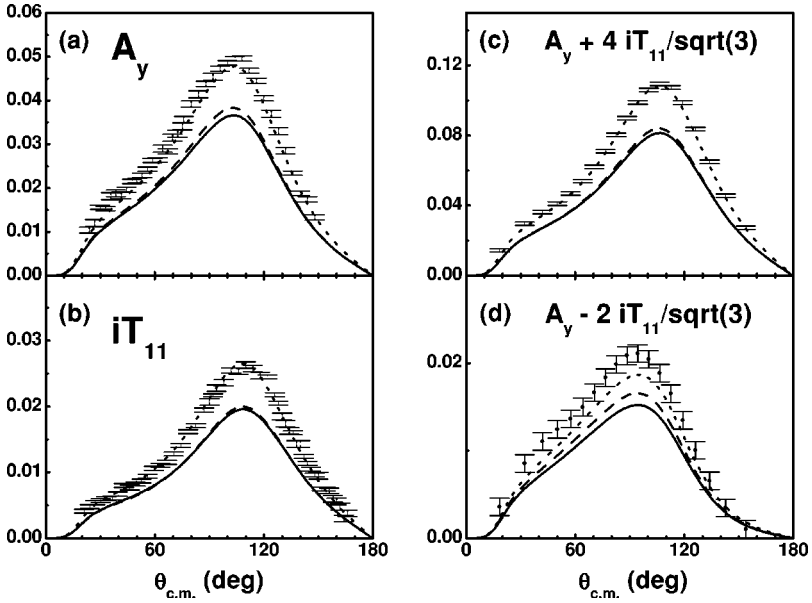

FIG. 4. Comparison of the Faddeev calculations and experimental data [3] for (a) the proton vector analyzing power A_y, (b) the deuteron vector analyzing power iT_{11}, (c) $A_y+(4/\sqrt{3})iT_{11}$, and (d) $A_y-(2/\sqrt{3})iT_{11}$ in the p-d scattering at $E_p=3$ MeV. The solid curves denote the calculations for AV18, the dashed curves for AV18+BR, and the dotted curves for AV18+BR+SO. For (c) and (d), quasiexperimental data made by fitting the experimental data of A_y and iT_{11} in Ref. [3] are plotted with the error bars.

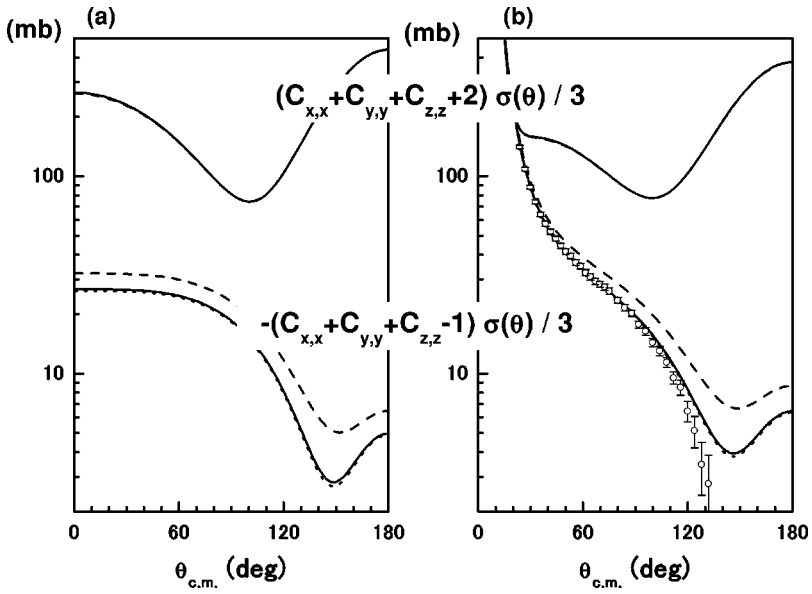

FIG. 5. Effects of 3NFs on spin correlation coefficients for vector polarizations of deuterons. The calculated $(C_{x,x}+C_{y,y}+C_{z,z}+2)\sigma(\theta)/3$ and $-(C_{x,x}+C_{y,y}+C_{z,z}-1)\sigma(\theta)/3$ are shown for the *n-d* and *p-d* scattering at $E_N=3$ MeV in (a) and (b), respectively, where the dashed curves denote the calculations for AV18, the solid curves for AV18+BR, and the dotted curves for AV18 +GS. See the text for the points with error bars.

$$\frac{1}{2}(C_{x,x}+C_{y,y})=\frac{1}{2N_R}\mathrm{Re}\Big\{-\frac{4}{3}|U_1|^2+\frac{2}{3}|U_3|^2-\frac{2\sqrt{2}}{3}U_1^*T_1(0)+\frac{2}{3}U_3^*T_2(0)-\frac{4}{3}U_3^*T_3(0)\Big\} \tag{25}$$

and the spin correlation coefficient for the longitudinal polarization $C_{z,z}$ in the SAD approximation is given by

$$C_{z,z}=\frac{1}{N_R}\mathrm{Re}\Big\{-\frac{2}{3}|U_1|^2+\frac{1}{3}|U_3|^2+\frac{2\sqrt{2}}{3}U_1^*T_1(0)-\frac{2}{3}U_3^*T_2(0)+\frac{4}{3}U_3^*T_3(0)\Big\}. \tag{26}$$

These results suggest that one can get $-2|U_1|^2+|U_3|^2$ in terms of the spin correlation observables by taking a linear combination of Eqs. (25) and (26). Further, by using the unpolarized differential cross section $\sigma(\theta)$, we get

$$|U_1|^2=-2(C_{x,x}+C_{y,y}+C_{z,z}-1)\sigma(\theta) \tag{27}$$

and

$$|U_3|^2=2(C_{x,x}+C_{y,y}+C_{z,z}+2)\sigma(\theta), \tag{28}$$

where we have used Eqs. (17) and (18) with Eq. (19).

For both of the *p-d* and *n-d* scattering, $-\frac{3}{2}(C_{x,x}+C_{y,y}+C_{z,z}-1)\sigma(\theta)$ and $\frac{3}{2}(C_{x,x}+C_{y,y}+C_{z,z}+2)\sigma(\theta)$ obtained by the full calculations are displayed in Fig. 5. These quantities describe $\frac{1}{6}|U_1|^2$ and $\frac{1}{6}|U_3|^2$, respectively, in the SAD approximation and we see again that $|U_3|^2$ is much larger than $|U_1|^2$ for the *n-d* scattering as in Fig. 1 and also for the *p-d* scattering except for small angles where the Coulomb interaction dominates. The contributions of the BR-3NF and the GS-3NF are displayed in the figure, where one can see that the contributions are remarkable in $|U_1|^2$ but not in $|U_3|^2$ and the GS-3NF is a good simulation of the scalar part of the BR-3NF. Such 3NF contributions will experimentally be examined by measuring the cross section and the spin correlation coefficients.

In Fig. 5(b), we plot the data of approximate doublet cross sections obtained by

$$\sigma_1(\theta)\equiv\sigma^{\mathrm{exp}}(\theta)-\frac{1}{6}|U_3^{\mathrm{cal}}|^2, \tag{29}$$

where the experimental data in Ref. [2] are used for $\sigma^{\mathrm{exp}}(\theta)$ and the results of the AV18+BR calculation for U_3^{cal}. Since the amplitude U_3 is little affected by the 3NFs as observed in Fig. 2, the use of another calculation for U_3^{cal} produces essentially the same results. The theoretical prediction of $-\frac{1}{3}(C_{x,x}+C_{y,y}+C_{z,z}-1)\sigma(\theta)$ agrees well with the data $\sigma_1(\theta)$ up to $\theta\sim120°$ when the 3NF is included, showing the 3NF contribution to be indispensable to describe the doublet scattering.

The remarkable effect of the 3NF on U_1 is related to the effect on the triton binding energy, as will be understood by the characteristic that the doublet scattering amplitudes at low energies are governed by a position of the 3N bound state pole [14]. Then it will be important to confirm such theoretical predictions of the characteristics of the *n-d* central interaction by the experimental measurements to fully understand the role of the scalar part of the 2πE-3NF at low energies. Other combinations of $C_{x,x}$, $C_{y,y}$, and $C_{z,z}$ will be discussed later together with tensor analyzing powers.

Further, we will examine $C_{x,z}$ and $C_{z,x}$ as other examples of the spin correlation coefficients for the vector polarizations of the nucleon and the deuteron. Generally, the contributions of the vector amplitudes and those of the tensor ones will be mixed up in these coefficients. However, their effects are separated from each other by considering their linear combinations. In fact, in the SAD approximation,

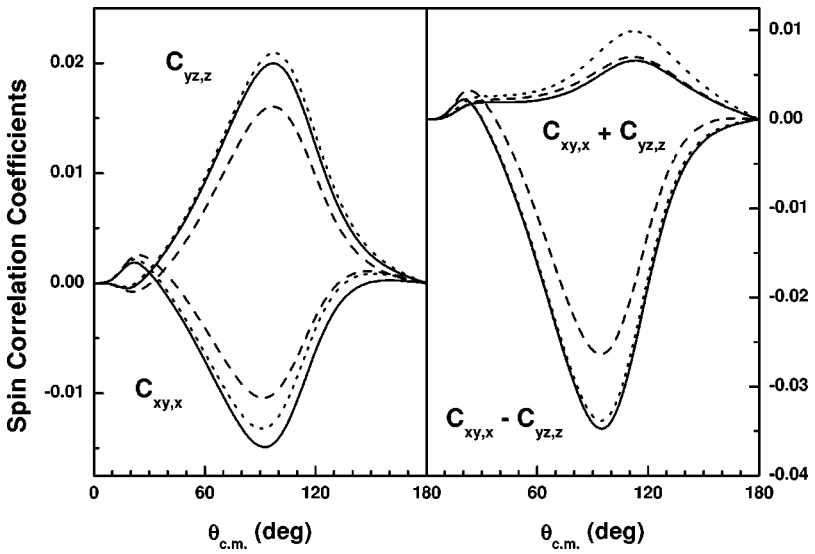

FIG. 6. Effects of 3NFs on the spin correlation coefficients $C_{xy,x}$ and $C_{yz,z}$, and their linear combinations $C_{xy,x}+C_{yz,z}$ and $C_{xy,x}-C_{yz,z}$ for the p-d scattering at $E_p=3$ MeV. The dashed curves denote the calculations for AV18, the solid curves for AV18+BR, and the dotted curves for AV18+BR+SO.

$$C_{x,z}+C_{z,x}=\frac{2}{\sqrt{3}N_R}\mathrm{Re}\{-2U_1^*T_1(1)+\sqrt{2}U_3^*(T_2(1)-2T_3(1))\}, \tag{30}$$

$$C_{x,z}-C_{z,x}=-\frac{2\sqrt{2}}{N_R}\mathrm{Re}\{(\sqrt{2}U_1-U_3)^*S_2\}. \tag{31}$$

The combination $C_{x,z}+C_{z,x}$ consists of the scalar amplitudes and the tensor ones and will reflect the contributions of the central interactions and the tensor ones. On the contrary, the combination $C_{x,z}-C_{z,x}$ will describe the contributions of the central interactions and the spin vector interactions. The former quantity will be investigated by considering further combinations with tensor analyzing powers. The latter quantity will exhibit the contribution of the SO-3NF to the vector amplitude S_2, since U_1 is small and U_3 is insensitive to the 3NF.

Next we will investigate $C_{xy,x}$ and $C_{yz,z}$ as examples of the spin correlation coefficients due to the tensor polarizations of the deuteron. In the SAD approximation,

$$C_{xy,x}+C_{yz,z}=\frac{3}{2}C_{yy,y}=\frac{2}{N_R}\mathrm{Im}\left\{-U_1(2\sqrt{2}S_1+S_2)^*+U_3\left(-\frac{1}{\sqrt{2}}S_2+\sqrt{\frac{2}{5}}S_3\right)^*\right\}, \tag{32}$$

$$C_{xy,x}-C_{yz,z}=-\left(C_{xx,y}+\frac{1}{2}C_{yy,y}\right)=\frac{2\sqrt{3}}{N_R}\mathrm{Im}\left\{U_1T_1(1)^*+\frac{1}{\sqrt{2}}U_3T_2(1)^*\right\}. \tag{33}$$

Due to Eqs. (32) and (33), $C_{xy,x}+C_{yz,z}$ characterizes the contribution of the vector amplitudes and $C_{xy,x}-C_{yz,z}$ that of the tensor ones. Further it is expected that the SO-3NF contributes to the former quantity through the vector amplitudes S_2 and S_3 and the BR-3NF to the latter through the tensor amplitude $T_2(1)$, since the magnitude of U_1 is small compared to that of U_3 and U_3 is hardly affected by the 3NF.

In Fig. 6, the calculated $C_{xy,x}$ and $C_{yz,z}$ and their linear combinations, $C_{xy,x}+C_{yz,z}$ and $C_{xy,x}-C_{yz,z}$ for the p-d scattering are displayed for the three kinds of interactions, AV18, AV18+BR, and AV18+BR+SO. In the calculated $C_{xy,x}$ and $C_{yz,z}$, the vector effect of the SO-3NF and the tensor effect of the BR-3NF are actually mixed up as seen in the left panel of Fig. 6. However, in the right panel of Fig. 6, they are clearly separated from each other, that is, the effect of the SO-3NF appears in $C_{xy,x}+C_{yz,z}$ but not in $C_{xy,x}-C_{yz,z}$, while the effect of the BR-3NF appears in the latter combination but not in the former one. These characteristics are consistent with the theoretical prediction by Eqs. (32) and (33). Therefore, measurements of these spin correlation coefficients will be useful to identify the contributions of these 3NF, separately.

D. Tensor analyzing powers of deuterons

Tensor analyzing powers of the deuteron $T_{2\kappa}$ ($\kappa=0,1,2$) are defined by

$$T_{2\kappa}=\frac{1}{N_R}\mathrm{Tr}(\boldsymbol{M}\tau_{2\kappa}\boldsymbol{M}^\dagger), \tag{34}$$

where $\tau_{2\kappa}$ is the spin tensor operator of the deuteron with the z component κ. In the SAD approximation,

$$T_{2\kappa}=\frac{1}{N_R}\mathrm{Re}\{-2U_1^*T_1(\kappa)+\sqrt{2}U_3^*(T_2(\kappa)+T_3(\kappa))\}. \tag{35}$$

Then, the tensor analyzing powers represent the contributions of the scalar amplitudes and the tensor ones. However, the tensor amplitudes are influenced by the tensor part of the BR-3NF, as shown in Fig. 2, where the magnitudes of $T_3(0)$ and $T_3(1)$ are affected by the 3NF at most angles, while the magnitude of $T_3(2)$ is not. Such 3NF effects can be ex-

tracted by the linear combination of the tensor analyzing powers and the spin correlation coefficients. Using Eqs. (25) and (26), we get in the SAD approximation,

$$\frac{1}{\sqrt{2}}(C_{x,x}+C_{y,y})-\sqrt{2}C_{z,z} = \frac{1}{N_R}\mathrm{Re}\{-2U_1^*T_1(0)+\sqrt{2}U_3^*(T_2(0)-2T_3(0))\}. \tag{36}$$

From Eqs. (35) and (36), we obtain

$$T_{20}-\frac{1}{\sqrt{2}}(C_{x,x}+C_{y,y})+\sqrt{2}C_{z,z}=\frac{3\sqrt{2}}{N_R}\mathrm{Re}(U_3^*T_3(0)). \tag{37}$$

Relations similar to Eq. (37) are derived for the tensor amplitudes $T_3(1)$ and $T_3(2)$ in the SAD approximation,

$$T_{21}-\frac{\sqrt{3}}{2}(C_{x,z}+C_{z,x})=\frac{3\sqrt{2}}{N_R}\mathrm{Re}(U_3^*T_3(1)), \tag{38}$$

$$T_{22}+\frac{\sqrt{3}}{2}(C_{x,x}-C_{y,y})=\frac{3\sqrt{2}}{N_R}\mathrm{Re}(U_3^*T_3(2)). \tag{39}$$

Since U_3 is insensitive to the 3NF, the right hand sides of Eqs. (37), (38), and (39) will reflect the tensor effect of the BR-3NF on $T_3(0)$, $T_3(1)$, and $T_3(2)$ shown in Fig. 2. To eliminate the 3NF effect on N_R, we will show the calculated $[T_{20}-(1/\sqrt{2})(C_{x,x}+C_{y,y})+\sqrt{2}C_{z,z}]\sigma(\theta)$, $[T_{21}-(\sqrt{3}/2)\times(C_{x,z}+C_{z,x})]\sigma(\theta)$, and $[T_{22}+(\sqrt{3}/2)(C_{x,x}-C_{y,y})]\sigma(\theta)$ in Fig. 7. The figure shows the 3NF tensor effects to be consistent with the characteristics of the effects on tensor amplitudes in Fig. 2. That is, the 3NF tensor effect is small but finite in $\mathrm{Re}(U_3^*T_3(0))$ and $\mathrm{Re}(U_3^*T_3(1))$, while the effect is almost negligible in $\mathrm{Re}(U_3^*T_3(2))$. These features can be examined by measuring the cross section and the spin correlation coefficients and such measurements will be important to determine the contribution of the 2NF tensor interactions and the 3NF tensor effect in the scattering, since $T_3(0)$, $T_3(1)$, and $T_3(2)$ form a complete set of the tensor amplitude in the spin quartet scattering.

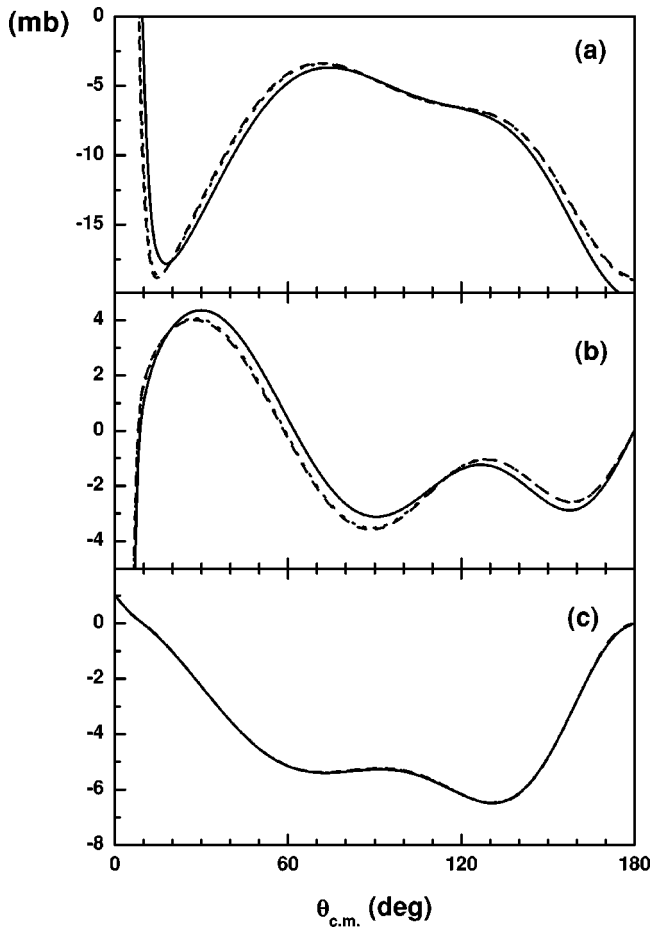

FIG. 7. Effects of 3NFs on tensor amplitudes in the p-d scattering at $E_p=3$ MeV. The quantities, $[T_{20}-(1/\sqrt{2})(C_{x,x}+C_{y,y})+\sqrt{2}C_{z,z}]\sigma(\theta)$, $[T_{21}-(\sqrt{3}/2)(C_{x,z}+C_{z,x})]\sigma(\theta)$, and $[T_{22}+(\sqrt{3}/2)(C_{x,x}-C_{y,y})]\sigma(\theta)$ (see text) are shown in (a), (b), and (c), respectively. The dashed curves denote the calculations for AV18, the solid curves for AV18+BR, and the dotted curves for AV18+GS. The dashed curves and the dotted curves are overlapped almost completely in (a) and (b), and the three kinds of curves cannot be identified to each other in (c).

V. CONCLUDING REMARKS

We have proposed some combinations of the scattering observables for obtaining the detailed information on the contributions of the 2NF and various models of the 3NF. Since each combination characterizes the contribution of a particular interaction, measurements of these quantities will provide clear tests for the validity of the interaction.

The numerical investigations are particularly focused on the contributions of the 2πE-3NF and the SO-3NF. As is well-known the 2πE-3NF provides an indispensable contribution to the triton binding energy, and by the present analyses it turns out that this 3NF effect produces clear contributions to the spin doublet scalar amplitude in the N-d scattering, which can be examined by measuring the cross section and some spin correlation coefficients. Further, the Faddeev calculations clarify that the 2πE-3NF contributes also as the tensor interaction to the tensor amplitudes in the spin quartet scattering. These 3NF effects will be criticized by comparing with experimental data when the related observables are measured. The SO-3NF produces the remarkable contribution to the vector amplitudes in the quartet scattering and also in the doublet-quartet nondiagonal transition. This improves the calculated vector analyzing powers of the proton and the deuteron successfully, although the agreement with the experimental data transformed for the nondiagonal transition is not so good as that for the spin quartet scattering.

The SAD approximation is useful to find the suitable combination of the spin observables for the examination of a particular interaction. In the present investigation, the analyzing powers and the spin correlation coefficients are chosen as the spin observables. However, polarization transfer

coefficients will also be available for the examination of the interaction. For the convenience of such applications, we will give in Appendix B the formulas of the polarization transfer coefficients in the SAD approximation, which will be useful in finding suitable combinations for testing of the validity of particular interactions.

ACKNOWLEDGMENTS

This research was supported by the Japan Society for the Promotion of Science, under Grant-in-Aids for Scientific Research No. 13640300. The numerical calculations were supported, in part, by the Computational Science Research Center, Hosei University, under Project No. lab0003.

APPENDIX A: MATRIX ELEMENTS OF *M* IN TERMS OF THE INVARIANT AMPLITUDES

The matrix elements $A,\ldots,R$ in Eq. (1) are described by the invariant amplitudes $U_1,\ldots,V(\kappa)$ as follows:

$$A=\frac{1}{2}[U_3+T_3(0)], \tag{A1}$$

$$B=\frac{1}{\sqrt{6}}[T_2(1)-T_3(1)]-\frac{1}{\sqrt{2}}S_4+\frac{1}{\sqrt{10}}S_3+\frac{1}{\sqrt{15}}V(1), \tag{A2}$$

$$C=-\frac{1}{\sqrt{3}}\left(\frac{1}{2}T_2(1)+T_3(1)\right)+\frac{1}{2}S_4+\frac{1}{\sqrt{5}}S_3+\sqrt{\frac{2}{15}}V(1), \tag{A3}$$

$$D=\frac{1}{\sqrt{3}}[-T_2(2)+T_3(2)-V(2)], \tag{A4}$$

$$E=\frac{1}{\sqrt{6}}[2T_2(2)+T_3(2)-V(2)], \tag{A5}$$

$$F=V(3), \tag{A6}$$

$$G=-\frac{1}{\sqrt{6}}[T_1(1)+T_3(1)]-\frac{1}{\sqrt{2}}S_2-\frac{1}{\sqrt{10}}S_3-\frac{1}{\sqrt{15}}V(1), \tag{A7}$$

$$H=\frac{\sqrt{2}}{3}U_1+\frac{1}{6}U_3+\frac{1}{6}[-2T_1(0)+2T_2(0)-T_3(0)], \tag{A8}$$

$$I=-\frac{1}{3}U_1+\frac{1}{3\sqrt{2}}U_3-\frac{1}{3\sqrt{2}}[2T_1(0)+T_2(0)+T_3(0)], \tag{A9}$$

$$J=\frac{1}{2\sqrt{3}}[2T_1(1)-T_2(1)]+\frac{\sqrt{2}}{3}S_1-\frac{1}{6}S_4-\frac{1}{3}S_2+\frac{2}{3\sqrt{5}}S_3-\sqrt{\frac{2}{15}}V(1), \tag{A10}$$

$$K=\frac{1}{\sqrt{6}}[T_1(1)+T_2(1)]-\frac{2}{3}S_1+\frac{1}{3\sqrt{2}}(S_4-S_2)+\frac{\sqrt{2}}{3\sqrt{5}}S_3-\frac{1}{\sqrt{15}}V(1), \tag{A11}$$

$$L=\frac{1}{\sqrt{6}}[-2T_1(2)+T_3(2)+V(2)], \tag{A12}$$

$$M=\frac{1}{2\sqrt{3}}[T_1(1)-2T_3(1)]+\frac{1}{2}S_2-\frac{1}{\sqrt{5}}S_3-\sqrt{\frac{2}{15}}V(1), \tag{A13}$$

$$N=\frac{1}{3\sqrt{2}}[-\sqrt{2}U_1+U_3+T_1(0)+2T_2(0)-T_3(0)], \tag{A14}$$

$$O=\frac{1}{3}\left(\frac{1}{\sqrt{2}}U_1+U_3+T_1(0)-T_2(0)-T_3(0)\right), \tag{A15}$$

$$P=-\frac{1}{\sqrt{6}}[T_1(1)+T_2(1)]-\frac{1}{3}S_1+\frac{1}{3\sqrt{2}}(-S_4+S_2)+\frac{2\sqrt{2}}{3\sqrt{5}}S_3-\frac{2}{\sqrt{15}}V(1), \tag{A16}$$

$$Q=\frac{1}{2\sqrt{3}}[-T_1(1)+2T_2(1)]+\frac{1}{6}(2\sqrt{2}S_1+2S_4+S_2)+\frac{2}{3\sqrt{5}}S_3-\sqrt{\frac{2}{15}}V(1), \tag{A17}$$

$$R=\frac{1}{\sqrt{3}}[T_1(2)+T_3(2)]+\frac{1}{\sqrt{3}}V(2). \tag{A18}$$

APPENDIX B: POLARIZATION TRANSFER COEFFICIENTS IN THE SAD APPROXIMATION

1. Deuteron (vector) to nucleon transfers

The polarization transfer coefficient is defined as

$$K_\alpha^\beta(d\text{-}n)=\frac{1}{N_R}\mathrm{Tr}(\boldsymbol{M}\tau_\alpha\boldsymbol{M}^\dagger\sigma_\beta). \tag{B1}$$

Define X_1, $Y_1(\kappa=0,1,2)$, and Z_1 by

$$X_1 \equiv -\frac{2}{3}|U_1|^2+\frac{5}{3}|U_3|^2-\frac{4\sqrt{2}}{3}\mathrm{Re}(U_1U_3^*), \tag{B2}$$

$$Y_1(\kappa)\equiv\frac{\sqrt{2}}{3}\mathrm{Re}\Big\{U_1(T_1(\kappa)-4T_2(\kappa)+2T_3(\kappa))^* + \sqrt{2}U_3\Big(T_1(\kappa)+\frac{1}{2}T_2(\kappa)+2T_3(\kappa)\Big)^*\Big\}, \tag{B3}$$

$$Z_1\equiv\mathrm{Re}\Big\{(\sqrt{2}U_1-U_3)\Big(S_1+\frac{5}{2\sqrt{2}}S_2+\sqrt{\frac{5}{2}}S_3\Big)^*\Big\}. \tag{B4}$$

Then we get

$$K_x^x(d\text{-}n)+K_y^y(d\text{-}n)=\frac{2}{3N_R}[X_1-Y_1(0)], \tag{B5}$$

$$K_z^z(d\text{-}n)=\frac{1}{3N_R}[X_1+2Y_1(0)], \tag{B6}$$

$$K_x^x(d\text{-}n)-K_y^y(d\text{-}n)=\frac{2\sqrt{2}}{\sqrt{3}N_R}Y_1(2), \tag{B7}$$

$$K_z^x(d\text{-}n)+K_x^z(d\text{-}n)=-\frac{2\sqrt{2}}{\sqrt{3}N_R}Y_1(1), \tag{B8}$$

$$K_z^x(d\text{-}n)-K_x^z(d\text{-}n)=\frac{8}{9N_R}Z_1. \tag{B9}$$

2. Nucleon to deuteron (vector) transfers

The polarization transfer coefficient is defined as

$$K_\alpha^\beta(n\text{-}d)=\frac{1}{N_R}\mathrm{Tr}(\boldsymbol{M}\sigma_\alpha\boldsymbol{M}^\dagger\tau_\beta). \tag{B10}$$

Define X_2, $Y_2(\kappa=0,1,2)$, and Z_2 as

$$X_2\equiv X_1, \tag{B11}$$

$$Y_2(\kappa)\equiv\frac{\sqrt{2}}{3}\mathrm{Re}\Big\{U_1(4T_1(\kappa)-T_2(\kappa)+2T_3(\kappa))^* + \sqrt{2}U_3\Big(-\frac{1}{2}T_1(\kappa)-T_2(\kappa)+2T_3(\kappa)\Big)^*\Big\}, \tag{B12}$$

$$Z_2\equiv Z_1. \tag{B13}$$

Then we get

$$K_x^x(n\text{-}d)+K_y^y(n\text{-}d)=\frac{2}{3N_R}[X_2-Y_2(0)], \tag{B14}$$

$$K_z^z(n\text{-}d)=\frac{1}{3N_R}[X_2+2Y_2(0)], \tag{B15}$$

$$K_x^x(n\text{-}d)-K_y^y(n\text{-}d)=\frac{2\sqrt{2}}{\sqrt{3}N_R}Y_2(2), \tag{B16}$$

$$K_z^x(n\text{-}d)+K_x^z(n\text{-}d)=-\frac{2\sqrt{2}}{\sqrt{3}N_R}Y_2(1), \tag{B17}$$

$$K_z^x(n\text{-}d)-K_x^z(n\text{-}d)=\frac{8}{9N_R}Z_2. \tag{B18}$$

3. Deuteron (tensor) to nucleon transfers

The polarization transfer coefficient is defined as

$$K_{\alpha\beta}^\gamma(d\text{-}n)=\frac{1}{N_R}\mathrm{Tr}(\boldsymbol{M}\tau_{\alpha\beta}\boldsymbol{M}^\dagger\sigma_\gamma). \tag{B19}$$

Define X_3, $Y_3(\kappa=0,1,2)$, and Z_3 as

$$X_3\equiv 0, \tag{B20}$$

$$Y_3(\kappa)\equiv\frac{2}{\sqrt{3}}\mathrm{Im}\Big\{U_1(T_1(\kappa)-2T_3(\kappa))^* + \sqrt{2}U_3\Big(T_1(\kappa)+\frac{3}{2}T_2(\kappa)+T_3(\kappa)\Big)^*\Big\}, \tag{B21}$$

$$Z_3\equiv\mathrm{Im}\Big\{U_1\Big(S_2-\frac{2}{\sqrt{5}}S_3\Big)^* - 2U_3\Big(S_1+\frac{3}{2\sqrt{2}}S_2-\sqrt{\frac{2}{5}}S_3\Big)^*\Big\}. \tag{B22}$$

Then we get

$$K_{xx}^y(d\text{-}n)-K_{yy}^y(d\text{-}n)=\frac{1}{N_R}[-Y_3(1)-2Z_3], \tag{B23}$$

$$K_{xx}^y(d\text{-}n)+K_{yy}^y(d\text{-}n)=\frac{1}{N_R}\Big(-Y_3(1)+\frac{2}{3}Z_3\Big), \tag{B24}$$

$$K_{xy}^z(d\text{-}n)=\frac{1}{N_R}Y_3(2), \tag{B25}$$

$$K_{yz}^z(d\text{-}n)=\frac{1}{N_R}\Big(-\frac{1}{2}Y_3(1)+Z_3\Big), \tag{B26}$$

$$K_{yz}^x(d\text{-}n)-K_{xz}^y(d\text{-}n)=-\frac{1}{N_R}\sqrt{\frac{3}{2}}Y_3(0). \tag{B27}$$

4. Nucleon to deuteron (tensor) transfers

The polarization transfer coefficient is defined as

$$K_\alpha^{\beta\gamma}(n\text{-}d)=\frac{1}{N_R}\mathrm{Tr}(\boldsymbol{M}\sigma_\alpha\boldsymbol{M}^\dagger\tau_{\beta\gamma}). \tag{B28}$$

Define X_4, $Y_4(\kappa=0,1,2)$, and Z_4 as

$$X_4\equiv 0, \tag{B29}$$

$$Y_4(\kappa)\equiv\frac{2}{\sqrt{3}}\mathrm{Im}\Big\{U_1(T_2(\kappa)+2T_3(\kappa))^* + \sqrt{2}U_3\Big(\frac{3}{2}T_1(\kappa)+T_2(\kappa)-T_3(\kappa)\Big)^*\Big\}, \tag{B30}$$

$$Z_4\equiv Z_3. \tag{B31}$$

Then we get

$$K_y^{xx}(n\text{-}d)-K_y^{yy}(n\text{-}d)=\frac{1}{N_R}[-Y_4(1)-2Z_4], \tag{B32}$$

$$K_y^{xx}(n\text{-}d)+K_y^{yy}(n\text{-}d)=\frac{1}{N_R}\Big(-Y_4(1)+\frac{2}{3}Z_4\Big), \tag{B33}$$

$$K_z^{xy}(n\text{-}d)=\frac{1}{N_R}Y_4(2), \tag{B34}$$

$$K_z^{yz}(n\text{-}d)=\frac{1}{N_R}\Big(-\frac{1}{2}Y_4(1)+Z_4\Big), \tag{B35}$$

$$K_x^{yz}(n\text{-}d)+K_y^{xz}(n\text{-}d)=-K_z^{xy}(n\text{-}d), \tag{B36}$$

$$K_x^{yz}(n\text{-}d)-K_y^{xz}(n\text{-}d)=-\frac{1}{N_R}\sqrt{\frac{3}{2}}Y_4(0). \tag{B37}$$

5. Deuteron (vector) to deuteron (vector) transfers

The polarization transfer coefficient is defined as

$$K_\alpha^{\beta}(d\text{-}d)=\frac{1}{N_R}\mathrm{Tr}(\boldsymbol{M}\tau_\alpha\boldsymbol{M}^\dagger\tau_{\beta}). \tag{B38}$$

Define X_5, $Y_5(\kappa=0,1,2)$, and Z_5 as

$$X_5\equiv\frac{4}{3}|U_1|^2+\frac{5}{3}|U_3|^2+\frac{2\sqrt{2}}{3}\mathrm{Re}(U_1U_3^*), \tag{B39}$$

$$Y_5(\kappa)\equiv\frac{4}{3}\mathrm{Re}\Big\{\sqrt{2}U_1\Big(T_1(\kappa)-T_2(\kappa)+\frac{1}{2}T_3(\kappa)\Big)^* + \frac{1}{2}U_3(T_1(\kappa)-T_2(\kappa)-4T_3(\kappa))^*\Big\}, \tag{B40}$$

$$Z_5\equiv\frac{4\sqrt{2}}{9}\mathrm{Re}\Big\{U_1\Big(4S_1+2\sqrt{2}S_2+\sqrt{\frac{5}{2}}S_3\Big)^* - U_3\Big(\frac{1}{\sqrt{2}}S_1+5S_2-\sqrt{5}S_3\Big)^*\Big\}. \tag{B41}$$

Then we get

$$K_x^x(d\text{-}d)+K_y^y(d\text{-}d)=\frac{1}{N_R}\Big(\frac{2}{3}X_5+\frac{1}{3}Y_5(0)\Big), \tag{B42}$$

$$K_x^x(d\text{-}d)-K_y^y(d\text{-}d)=-\frac{1}{N_R}\sqrt{\frac{2}{3}}Y_5(2), \tag{B43}$$

$$K_x^z(d\text{-}d)+K_z^x(d\text{-}d)=\frac{1}{N_R}\sqrt{\frac{2}{3}}Y_5(1), \tag{B44}$$

$$K_x^z(d\text{-}d)-K_z^x(d\text{-}d)=\frac{1}{N_R}Z_5, \tag{B45}$$

$$K_z^z(d\text{-}d)=\frac{1}{3N_R}[X_5-Y_5(0)]. \tag{B46}$$

6. Deuteron (vector) to deuteron (tensor) transfers

The polarization transfer coefficient is defined as

$$K_\alpha^{\beta\gamma}(d\text{-}d)=\frac{1}{N_R}\mathrm{Tr}(\boldsymbol{M}\tau_\alpha\boldsymbol{M}^\dagger\tau_{\beta\gamma}). \tag{B47}$$

Define X_6, $Y_6(\kappa=0,1,2)$, and Z_6 as

$$X_6\equiv 0, \tag{B48}$$

$$Y_6(\kappa)\equiv\sqrt{\frac{2}{3}}\mathrm{Im}\{\sqrt{2}U_1(2T_2(\kappa)+T_3(\kappa))^* + U_3(-3T_1(\kappa)+T_2(\kappa)+2T_3(\kappa))^*\}, \tag{B49}$$

$$Z_6\equiv\mathrm{Im}\Big\{U_1\Big(2S_2-\frac{1}{\sqrt{5}}S_3\Big)^*-U_3\Big(S_1+\frac{2\sqrt{2}}{\sqrt{5}}S_3\Big)^*\Big\}. \tag{B50}$$

Then we get

$$K_y^{xx}(d\text{-}d)+K_y^{yy}(d\text{-}d)=\frac{1}{N_R}\Big[Y_6(1)-\frac{2}{3}Z_6\Big], \tag{B51}$$

$$K_y^{xx}(d\text{-}d)-K_y^{yy}(d\text{-}d)=\frac{1}{N_R}[Y_6(1)+2Z_6], \tag{B52}$$

$$K_x^{xy}(d\text{-}d)=-\frac{1}{2}[K_y^{xx}(d\text{-}d)-K_y^{yy}(d\text{-}d)], \tag{B53}$$

$$K_y^{xz}(d\text{-}d)+K_x^{yz}(d\text{-}d)=\frac{1}{N_R}Y_6(2), \tag{B54}$$

$$K_y^{xz}(d\text{-}d)-K_x^{yz}(d\text{-}d)=-\frac{1}{N_R}\sqrt{\frac{3}{2}}Y_6(0), \tag{B55}$$

$$K_z^{xy}(d\text{-}d)=-\frac{1}{N_R}Y_6(2), \tag{B56}$$

$$K_z^{yz}(d\text{-}d)=\frac{1}{N_R}\left(\frac{1}{2}Y_6(1)-Z_6\right). \tag{B57}$$

7. Deuteron (tensor) to deuteron (vector) transfers

The polarization transfer coefficient is defined as

$$K_{\alpha\beta}^{\gamma}(d\text{-}d)=\frac{1}{N_R}\mathrm{Tr}(\boldsymbol{M}\tau_{\alpha\beta}\boldsymbol{M}^{\dagger}\tau_{\gamma}). \tag{B58}$$

Define X_7, $Y_7(\kappa=0,1,2)$, and Z_7 as

$$X_7\equiv 0, \tag{B59}$$

$$Y_7(\kappa)\equiv\sqrt{\frac{2}{3}}\mathrm{Im}\{\sqrt{2}U_1(2T_1(\kappa)-T_3(\kappa))^* + U_3(T_1(\kappa)-3T_2(\kappa)-2T_3(\kappa))^*\}, \tag{B60}$$

$$Z_7\equiv Z_6. \tag{B61}$$

Then we get

$$K_{xx}^{y}(d\text{-}d)+K_{yy}^{y}(d\text{-}d)=\frac{1}{N_R}\left(Y_7(1)-\frac{2}{3}Z_7\right), \tag{B62}$$

$$K_{xx}^{y}(d\text{-}d)-K_{yy}^{y}(d\text{-}d)=\frac{1}{N_R}[Y_7(1)+2Z_7], \tag{B63}$$

$$K_{xy}^{x}(d\text{-}d)=-\frac{1}{2}[K_{xx}^{y}(d\text{-}d)-K_{yy}^{y}(d\text{-}d)], \tag{B64}$$

$$K_{xz}^{y}(d\text{-}d)+K_{yz}^{x}(d\text{-}d)=-K_{xy}^{z}(d\text{-}d)=\frac{1}{N_R}Y_7(2), \tag{B65}$$

$$K_{xz}^{y}(d\text{-}d)-K_{yz}^{x}(d\text{-}d)=-\frac{1}{N_R}\sqrt{\frac{3}{2}}Y_7(0), \tag{B66}$$

$$K_{yz}^{z}(d\text{-}d)=\frac{1}{N_R}\left(\frac{1}{2}Y_7(1)-Z_7\right). \tag{B67}$$

8. Nucleon to nucleon transfers

The polarization transfer coefficient is defined as

$$K_{\alpha}^{\beta}(n\text{-}n)=\frac{1}{N_R}\mathrm{Tr}(\boldsymbol{M}\sigma_{\alpha}\boldsymbol{M}^{\dagger}\sigma_{\beta}). \tag{B68}$$

Define X_8, $Y_8(\kappa=0,1,2)$, and Z_8 as

$$X_8\equiv\frac{1}{3}|U_1|^2+\frac{5}{3}|U_3|^2+\frac{8\sqrt{2}}{3}\mathrm{Re}(U_1U_3^*), \tag{B69}$$

$$Y_8(\kappa)\equiv\frac{4}{3}\mathrm{Re}\{(\sqrt{2}U_1-U_3)[T_1(\kappa)-T_2(\kappa)+2T_3(\kappa)]^*\}, \tag{B70}$$

$$Z_8\equiv\frac{8}{9}\mathrm{Re}\left\{U_1\left(\sqrt{\frac{1}{2}}S_1+2S_2+2\sqrt{5}S_3\right)^* - U_3\left(2S_1-5\sqrt{2}S_2-\sqrt{\frac{5}{2}}S_3\right)^*\right\}. \tag{B71}$$

Then we get

$$K_x^{x}(n\text{-}n)-K_y^{y}(n\text{-}n)=-\frac{1}{N_R}\sqrt{\frac{2}{3}}Y_8(2), \tag{B72}$$

$$K_x^{x}(n\text{-}n)+K_y^{y}(n\text{-}n)=\frac{1}{N_R}\left(\frac{2}{3}X_8+\frac{1}{3}Y_8(0)\right), \tag{B73}$$

$$K_z^{z}(n\text{-}n)=\frac{1}{3N_R}[X_8-Y_8(0)], \tag{B74}$$

$$K_x^{z}(n\text{-}n)+K_z^{x}(n\text{-}n)=\frac{1}{N_R}\sqrt{\frac{2}{3}}Y_8(1), \tag{B75}$$

$$K_x^{z}(n\text{-}n)-K_z^{x}(n\text{-}n)=\frac{1}{N_R}Z_8. \tag{B76}$$

9. Deuteron (tensor) to deuteron (tensor) transfers

The polarization transfer coefficient is defined as

$$K_{\alpha\beta}^{\gamma\delta}(d\text{-}d)=\frac{1}{N_R}\mathrm{Tr}(\boldsymbol{M}\tau_{\alpha\beta}\boldsymbol{M}^{\dagger}\tau_{\gamma\delta}). \tag{B77}$$

Define X_9, $Y_9(\kappa=0,1,2)$, and Z_9 as

$$X_9\equiv\frac{1}{2}|U_3|^2+\sqrt{2}\mathrm{Re}(U_1U_3^*), \tag{B78}$$

$$Y_9(\kappa)\equiv\mathrm{Re}\{\sqrt{2}U_1T_3(\kappa)^*-U_3(T_1(\kappa)-T_2(\kappa))^*\}, \tag{B79}$$

$$Z_9\equiv\mathrm{Re}\left\{\frac{3}{\sqrt{5}}U_1S_3^*+U_3\left(S_1-\sqrt{2}S_2+\sqrt{\frac{2}{5}}S_3\right)^*\right\}. \tag{B80}$$

Then we get

$$K_{zz}^{zz}(d\text{-}d)=[K_{xx}^{xx}(d\text{-}d)+K_{xx}^{yy}(d\text{-}d)]+[K_{yy}^{xx}(d\text{-}d)+K_{yy}^{yy}(d\text{-}d)] = \frac{2}{N_R}[X_9-Y_9(0)], \tag{B81}$$

$$-[K_{xx}^{xx}(d\text{-}d)+K_{xx}^{yy}(d\text{-}d)]+[K_{yy}^{xx}(d\text{-}d)+K_{yy}^{yy}(d\text{-}d)] = \frac{2\sqrt{6}}{N_R}Y_9(2), \tag{B82}$$

$$[K_{xx}^{xx}(d\text{-}d)-K_{xx}^{yy}(d\text{-}d)]+[K_{yy}^{xx}(d\text{-}d)-K_{yy}^{yy}(d\text{-}d)] = -\frac{2\sqrt{6}}{N_R}Y_9(2), \tag{B83}$$

$$[K_{xx}^{xx}(d\text{-}d)-K_{xx}^{yy}(d\text{-}d)]-[K_{yy}^{xx}(d\text{-}d)-K_{yy}^{yy}(d\text{-}d)] = \frac{6}{N_R}[X_9+Y_9(0)], \tag{B84}$$

$$K_{xy}^{xy}(d\text{-}d)=\frac{3}{2N_R}[X_9+Y_9(0)], \tag{B85}$$

$$K_{xz}^{xz}(d\text{-}d)+K_{yz}^{yz}(d\text{-}d)=\frac{3}{N_R}\left(X_9-\frac{1}{2}Y_9(0)\right), \tag{B86}$$

$$K_{xz}^{xz}(d\text{-}d)-K_{yz}^{yz}(d\text{-}d)=\frac{3}{N_R}\sqrt{\frac{3}{2}}Y_9(2), \tag{B87}$$

$$K_{yz}^{xy}(d\text{-}d)=\frac{3}{2N_R}\left(\sqrt{\frac{3}{2}}Y_9(1)-Z_9\right), \tag{B88}$$

$$K_{xz}^{xx}(d\text{-}d)-K_{xz}^{yy}(d\text{-}d)=\frac{3}{N_R}\left(\sqrt{\frac{3}{2}}Y_9(1)-Z_9\right), \tag{B89}$$

$$K_{xz}^{xx}(d\text{-}d)+K_{xz}^{yy}(d\text{-}d)=-\frac{1}{N_R}\left(\sqrt{\frac{3}{2}}Y_9(1)+3Z_9\right), \tag{B90}$$

$$K_{xx}^{xz}(d\text{-}d)+K_{yy}^{xz}(d\text{-}d)=\frac{1}{N_R}\left(-\sqrt{\frac{3}{2}}Y_9(1)+3Z_9\right), \tag{B91}$$

$$K_{xx}^{xz}(d\text{-}d)-K_{yy}^{xz}(d\text{-}d)=\frac{3}{N_R}\left(\sqrt{\frac{3}{2}}Y_9(1)+Z_9\right), \tag{B92}$$

$$K_{xy}^{yz}(d\text{-}d)=\frac{1}{2}[K_{xx}^{xz}(d\text{-}d)-K_{yy}^{xz}(d\text{-}d)]. \tag{B93}$$

[1] W. Glöckle, H. Witała, D. Hüber, H. Kamada, and J. Golak, Phys. Rep. **274**, 107 (1996).

[2] K. Sagara, H. Oguri, S. Shimizu, K. Maeda, H. Nakamura, T. Nakashima, and S. Morinobu, Phys. Rev. C **50**, 576 (1994).

[3] S. Shimizu, K. Sagara, H. Nakamura, K. Maeda, T. Miwa, N. Nishimori, S. Ueno, T. Nakashima, and S. Morinobu, Phys. Rev. C **52**, 1193 (1995).

[4] N. Sakamoto, H. Okamura, T. Uesaka, S. Ishida, H. Otsu, T. Wakasa, Y. Satou, T. Niizeki, K. Katoh, T. Yamashita, K. Hatanaka, Y. Koike, and H. Sakai, Phys. Lett. B **367**, 60 (1996).

[5] E. J. Stephenson, H. Witała, W. Glöckle, H. Kamada, and A. Nogga, Phys. Rev. C **60**, 061001(R) (1999).

[6] R. Bieber, W. Glöckle, J. Golak, M. N. Harakeh, D. Hüber, H. Huisman, N. Kalantar-Nayestanaki, H. Kamada, J. G. Messchendorp, A. Nogga, H. Sakai, N. Sakamomto, M. Seip, M. Volkerts, S. Y. van der Werf, and H. Witała, Phys. Rev. Lett. **84**, 606 (2000).

[7] H. Sakai, K. Sekiguchi, H. Witała, W. Glöckle, M. Hatano, H. Kamada, H. Kato, Y. Maeda, A. Nogga, T. Ohnishi, H. Okamura, N. Sakamoto, S. Sakoda, Y. Satou, K. Suda, A. Tamii, T. Uesaka, T. Wakasa, and K. Yako, Phys. Rev. Lett. **84**, 5288 (2000).

[8] R. V. Cadman, J. Brack, W. J. Cummings, J. A. Fedchak, B. D. Fox, H. Gao, W. Glöckle, J. Golak, C. Grosshauser, R. J. Holt, C. E. Jones, H. Kamada, E. R. Kinney, M. A. Miller, W. Nagengast, A. Nogga, B. R. Owen, K. Rith, E. Schmidt, E. C. Schulte, J. Sowinski, E. Sperisen, E. L. Thorsland, R. Tobey, J. Wilbert, and H. Witała, Phys. Rev. Lett. **86**, 967 (2001).

[9] C. R. Brune, W. H. Geist, H. J. Karwowski, E. J. Ludwig, K. D. Veal, M. H. Wood, A. Kievsky, S. Rosati, and M. Viviani, Phys. Rev. C **63**, 044013 (2001).

[10] K. Ermisch, A. M. van den Berg, R. Bieber, W. Glöckle, J. Golak, M. Hagemann, V. M. Hannen, M. N. Harakeh, M. A. de Huu, N. Kalantar-Nayestanaki, H. Kamada, M. Kiš, J. Kuroś-Żołnierczuk, M. Mahjour-Schafiei, A. Micherdzińska, A. Nogga, R. Skibiński, H. Witała, and H. J. Wörtche, Phys. Rev. Lett. **86**, 5862 (2001).

[11] M. H. Wood, C. R. Brune, B. M. Fisher, H. J. Karwowski, D. S. Leonard, E. J. Ludwig, A. Kievsky, S. Rosati, and M. Viviani, Phys. Rev. C **65**, 034002 (2002).

[12] K. Sekiguchi, H. Sakai, H. Witała, W. Glöckle, J. Golak, M. Hatano, H. Kamada, H. Kato, Y. Maeda, J. Nishikawa, A. Nogga, T. Ohnishi, H. Okamura, N. Sakamoto, S. Sakoda, Y. Satou, K. Suda, A. Tamii, T. Uesaka, T. Wakasa, and K. Yako, Phys. Rev. C **65**, 034003 (2002).

[13] J. E. McAninch, L. O. Lamm, and W. Haeberli, Phys. Rev. C **50**, 589 (1994).

[14] S. Ishikawa, Phys. Rev. C **59**, R1247 (1999).

[15] H. Witała, W. Glöckle, J. Golak, A. Nogga, H. Kamada, R. Skibiński, and J. Kuroś-Żołnierczuk, Phys. Rev. C **63**, 024007 (2001).

[16] A. Kievsky, M. Viviani, and S. Rosati, Phys. Rev. C **64**, 024002 (2001).

[17] Y. Koike and J. Haidenbauer, Nucl. Phys. **A463**, 365c (1987).

[18] H. Witała, W. Glöckle, and T. Cornelius, Nucl. Phys. **A491**, 157 (1988).

[19] H. Witała, W. Glöckle, D. Hüber, J. Golak, and H. Kamada, Phys. Rev. Lett. **81**, 1183 (1998).

[20] S. Ishikawa, M. Tanifuji, and Y. Iseri, Phys. Rev. C **64**, 024001 (2001).

[21] M. Tanifuji and K. Yazaki, Prog. Theor. Phys. **40**, 1023 (1968).

[22] S. Ishikawa, nucl-th/0206064.

[23] B. Jenny, W. Grüebler, P. A. Schmelzbach, V. König, and H. R. Rürgi, Nucl. Phys. **A337**, 77 (1980).
[24] S. Ishikawa, Nucl. Phys. **A463**, 145c (1987).
[25] R. B. Wiringa, V. G. J. Stoks, and R. Schiavilla, Phys. Rev. C **51**, 38 (1995).
[26] A. Kievsky, M. Viviani, and S. Rosati, Phys. Rev. C **52**, R15 (1995).
[27] R. B. Wiringa, R. A. Smith, and T. L. Ainsworth, Phys. Rev. C **29**, 1207 (1984).
[28] D. Hüber, W. Glöckle, J. Golak, H. Witała, H. Kamada, A. Kievsky, S. Rosati, and M. Viviani, Phys. Rev. C **51**, 1100 (1995).
[29] A. Kievsky, J. L. Friar, G. L. Payne, S. Rosati, and M. Viviani, Phys. Rev. C **63**, 064004 (2001).
[30] H. T. Coelho, T. K. Das, and M. R. Robilotta, Phys. Rev. C **28**, 1812 (1983).
[31] A. Kievsky, Phys. Rev. C **60**, 034001 (1999).